Master Thesis Work

Sensing of particles, micro-organisms and biomarkers using the camera of a mobile phone

Supervisor: Valerio Pruneri
Melanie Cazaban
Master in Photonics

UNIVERSITAT POLITÈCNICA DE CATALUNYA

UNIVERSITÉ TOULOUSE III PAUL SABATIER

ICFO The Institute of Photonic Sciences

UNIVERSITAT DE BARCELONA

UAB Universitat Autònoma de Barcelona

September 5, 2017

Abstract: We demonstrate a simple method to shape an incoherent light source in periodic patterns of the type of $\cos^{2n}(k_x x)\cos^{2m}(k_y y)$ by using pairs of birrefringent crystals known as Savart Plates. These patterns scalable and show reduced diffraction from obstacles.

References and links

1. Saxena, Manish and Eluru, Gangadhar and Gorthi, Sai Siva, "Structured illumination microscopy", Advances in optics an photonics, **7** (2). pp. 241–275 (2015).
2. M.G.L Gustafsson,"Surpassing the lateral resolution limit by a factor of two using structured illumination microscopy", J.Microsc, **198,** 82–87 (2000).
3. Schermelleh L, Heintzmann R, Leonhardt H,"A guide to super-resolution fluorescence microscopy", The Journal of Cell Biology, **190,** 165–175 (2010).
4. J. Geng,"Structured-light 3D surface imaging:a tutorial", Adv. Opt. Photon, **3,** 128–160 (2011).
5. Rego, Elizabeth and Shao, Lin,"Practical Structured Illumination Microscopy", Methods in molecular biology (Clifton, N.J.), **1251,** 175–92 (2015).
6. J.Durnin J.J Miceli, J.H Eberly,"Diffraction-Free Beams", Physical Review Letters, **58,** 1499–1501 (1987).
7. Carlos Lopez-Mariscal,Miguel A. Bandres,Julio Cesar Gutierrez-Vega,"Observation of the experimental propagation properties of Helmholtz-Gauss beams", Optical Engineering, **45,**(2006).
8. David McGloin and Kishan Dholakia,"Bessel Beams: Diffraction in a new light",Contemp Phys, **46,** 15–28 (2005).
9. Ricardez-Vargas and K. Volke-Sepulveda,"Experimental generation and dynamical reconfiguration of different circular optical lattices for applications in atom trapping",J. Opt. Soc. Am. B, **27,** 948-955 (2010).
10. R. J. Hernandez-Hernandez, R. A. Terborg, I. Ricardez-Vargas, and K. Volke-Sepulveda,"Experimental generation of MathieuGauss beams with a phase-only spatial light modulator",Appl. Opt. , **49,** 6903–6909 (2010).
11. Kimberly L. Berkowski, Kyle N. Plunkett, Qing Yu and Jeffrey S. Moore,"Introduction to Photolithography: Preparation of Microscale Polymer Silhouettes ",J. Chem. Educ., **82,** (9), p 1365 (2005).
12. Feng Chen, Zefang Deng, Qing Yang, Hao Bian, Guangqing Du, Jinhai Si, and Xun Hou,"Rapid fabrication of a large-area close-packed quasi-periodic microlens array on BK7 glass",Opt. Lett.., **39,** 606–609 (2014).

1. Introduction

Super-resolution imaging methods such as structured illumination microscopy[1] have offered various compromises between spatial resolution beyond the diffraction limit[2][3], imaging speed, and biocompatibility. It has become more important in new 3D imaging techniques, of both micro and macroscopic objects[4]. For applications such as fluorescence microscopy[5] or surface patterning it is interesting to simultaneously illuminate different and very well defined sites in a periodic array. This way it allows to minimise interactions between different zone, as well as mechanical robustness against external perturbations. To create the most homogeneous patterns the use of a low coherence light seems to be the best option. Due to the short coherence length the patterns present low noise due to optical element reflections. Most structured illumination methods involve coherent light sources where the setups are subjected to perturbations. The setups are very sensitive to turbulence and mechanical vibrations or amplitude modulation which in turn shows changes in the original pattern due to diffraction. To reduce these perturbations we propose a method based on an interferometric reader device. The main components of this device are two birefringent crystals known as Savart Plates.

2. Description of the structured illumination device components.

A Savart plate and a polarizing beam splitter work on a similar principle. The two orthogonally polarized beams travel parallel but with a lateral displacement given by the birefringent crystal without a phase delay between them. In order to get the best periodic patterns, the choice of an appropriate wavefront is essential.An original curved wavefront can be displaced from its original position with a distance S and so we can obtain an overlap region between the wavefronts as shown on Figure 1.

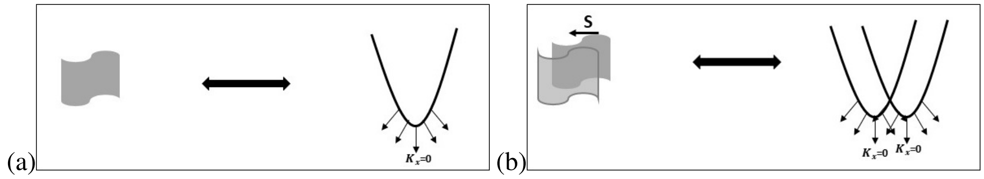

Fig. 1. (a).Scheme of a curved wavefront with K_x as the horizontal component of the wavenumber of the wavefront.(b).Scheme of the superposition of two wavefronts with a spatial displacement of the distance S.

When the input beam is linearly polarized a Savart plate will transform the distance S into changes in the polarization state. If we combine a polarisation analyser to a Savart Plate we can relate the polarization distribution to an interferometric intensity pattern. Super-resolution imaging methods such as structured illumination microscopy is based on the use of a periodic illumination pattern type. In 1D the illumination intensity would be:

$$I_n = I_0[cos(k_s x)]^{2n} \tag{1}$$

where:

$$k_s = \frac{\pi}{L} \tag{2}$$

With n an integer and I_0 corresponds to the maximum of the intensity and L the distance between each intensity peak. With the study of the Fourier spectrum of $\cos^n(k_s x)$ signals we noticed that the intensities of the structured illumination result from the superposition of 2n+1 plane waves. In the case of n=2 the analysis of the Fourier spectrum would give:

$$F_x[cos^n(k_s x)](K_x) = \frac{1}{2}\sqrt{\frac{\pi}{2}}[\delta(K_x - 2k_s) + 2\delta(K_x) + \delta(K_x + 2k_s)] \tag{3}$$

The wavenumbers of the plane waves differ from each other by an integer multiple of $2k_s$. The wavenumber of the normal incidence wave is K_x=0. If the component K_x is different of 0 then the amplitude of each wave decreases. To get a spectral composition we want,we locally approximate each curved wavefront as plane wave. We superpose curved wavefronts with a uniform intensity along a transverse displacement. The Figure 1.a shows this displacement from the first shear to the second shear(Figure 1.b).These displacements must be integer multiples of S with waves amplitudes modulated by the binominal coefficients. The shape of the wavefront is parabolic:

$$\phi(x) = \frac{\alpha}{2}x^2 + \phi_0 \tag{4}$$

A spatial displacement S along x of the wavefront $\phi(x)$ where ϕ_0 is an arbitrary phase offset and α sets the variation of the wavenumbers due to the displacement of the wavefront. This leads to the condition where:

$$2k_s = K_x(x \pm S) - K_x(x) = \frac{2\pi}{\lambda}\alpha S \tag{5}$$

with λ corresponds to the wavelength of the LED light source used. In two dimensions the wavefront would be a paraboloid. We get a pattern of the type of $\cos^n(k_s x)$ as shown on Figure 2, using a sequence of n Savart plates and n+1 intercalated polarizers(see Figure 3).

By approximating the paraboloidal wavefronts as spherical it is possible to obtain a given pattern periodicity by changing the radius of curvature:

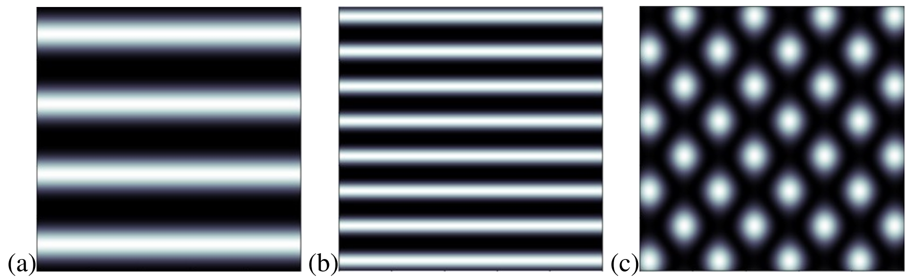

Fig. 2. Simulated intensity of a pattern of the type of $\cos^n(k_s x)$.
(a).For n=1 : $\cos^2(k_s x)$.
(b).For n=2 : $\cos^4(k_s x)$.
(c).Simulated intensity of a pattern in two dimension for n=1 $\cos^2(k_s x)\cos^2(k_s y)$.

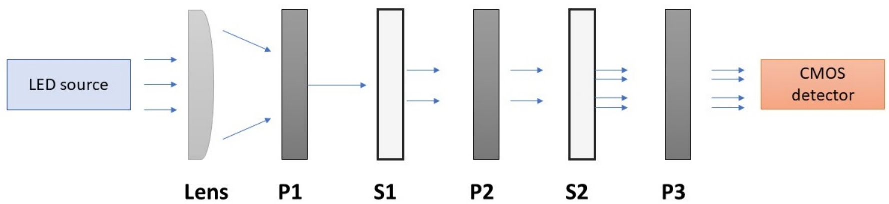

Fig. 3. Scheme of the intercalated Savart Plates and polarizers device, for the case n=2.

$$R(L) = \frac{LS}{\lambda} \tag{6}$$

The periodicity pattern is proportional to the propagation distance. The spherical wavefronts preserve the structure of the patterns. There are no limits to a given z-region of overlap beam unlike for a plane wave interference or any other propagation invariant beams[6]–[10].

3. Experimental setup and its applications.

3.1. Presentation of the setup.

The device that has been set up to create periodic patterns was made of a LED source, a lens, three polarizers and two Savart plates. The structured illumination setup is shown on Figure 4. At the output of the device a CMOS camera ThorLabs was used to record and observe the illumination.

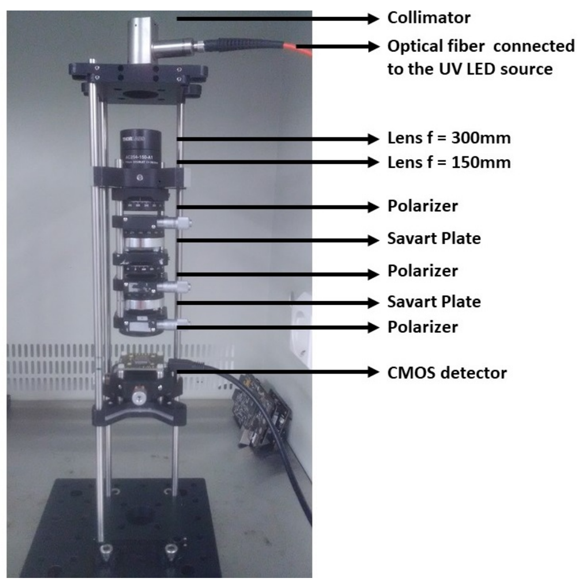

Fig. 4. Layout of the experimental setup.

In order to obtain the best pattern to work with, we investigated different configuration through a simulation program(see Figure 2). Then we reproduced them in the experiment. We fixed the polarizers and Savart Plates positions. Then we performed the measurements for four different wavelength LED light sources as shown on Figure 5.

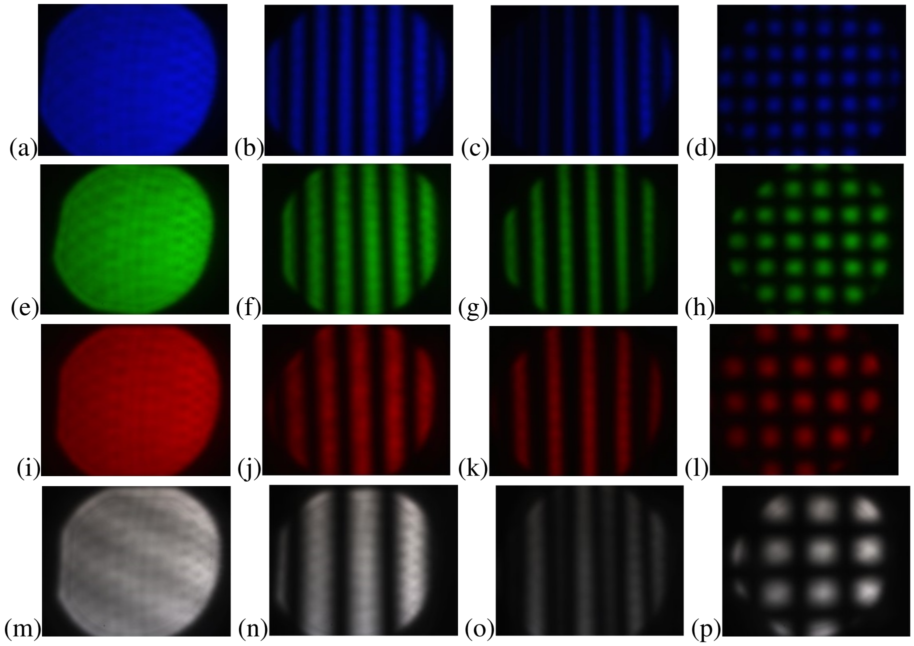

Fig. 5. CMOS detector images of the pattern at differents LED source wavelength.
LED source at 455nm: (a).Illumination of a uniform pattern.(b).I=$\cos^2(k_s x)$.(c).I=$\cos^4(k_s x)$.(d).I=$\cos^2(k_s x)\cos^2(k_s y)$.
LED source at 530nm: (e).Illumination of a uniform pattern.(f).I=$\cos^2(k_s x)$.(g).I=$\cos^4(k_s x)$.(h).I=$\cos^2(k_s x)\cos^2(k_s y)$.
LED source at 625nm: (i).Illumination of a uniform pattern.(j).I=$\cos^2(k_s x)$.(k).I=$\cos^4(k_s x)$.(l).I=$\cos^2(k_s x)\cos^2(k_s y)$.
LED source at 850nm: (m).Illumination of a uniform pattern.(n).I=$\cos^2(k_s x)$.(o).I=$\cos^4(k_s x)$.(p).I=$\cos^2(k_s x)\cos^2(k_s y)$.

By changing the direction of the crystals, different type of patterns were obtained. The first step was to align the polarisers and Savart Plates in a way to create a uniform illumination as shown on Figures 5a,e,i,m. It allowed us to note that the illumination beam was not homogeneously distributed. After several test of each element of the device it was found that the UV LED source was the main source of this irregularity. To rectify that, two option were considered: to modify the type of collimator used and to compensate with the exposure time. When the displacement was made along the same direction, the width of the obtained fringes changed (for instance see Figures 5b. and c.). Dotted pattern were obtained when the beam displacements occurred in orthogonal directions(see Figures 5c.). According to the measurements we made, we observed similar results to the simulation we did (see Figure 2). It means that by the analysis of the Fourier series of a given periodic pattern, the spectrum is the result of a sequence of crystals with different displacements.

3.2. Integration of the setup into the photolithography technique.

It is by using the photolithography method[11] that we chose to demonstrate the value of our structured illumination device. The first step of photolithography process was to deposit a photoresist on a substrate as a wafer or a slide of glass. The Spin coating technique was used to deposit a thin and uniform photoresist layer on slides of glass as shown on Figure 6. After replacing the LED source by a UV LED source, the photoresist samples were exposed. When a photoresist sample is exposed to a light radiation, it is necessary to use a mask. A mask is made of opaque and transparent sections which allow to define a desired pattern. In our case, we used our device as a mask because the pattern created was composed of dark and bright zones.

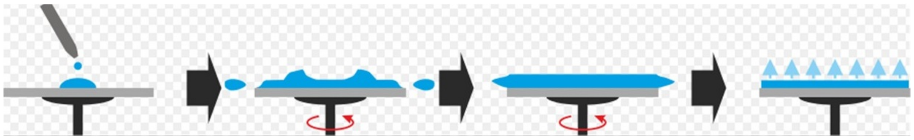

Fig. 6. Simplified scheme of the Spin coating technique

In order to ensure a perfect reproduction of the mask on the substrat, the photoresist had to react to the UV source with a certain exposure time condition. Once the chosen pattern was created by fixing the direction of the polarizers and Savart Plates, a first sample was exposed to the source at different exposure time. Then the substrat was developed by using a solvent that removed all the unexposed photoresist as shown on Figure 7. Under the exposure time of 120min the photoresist was not fully developed. But over 180min it was over exposed, the ideal exposure time would have been between 120min and 180min.

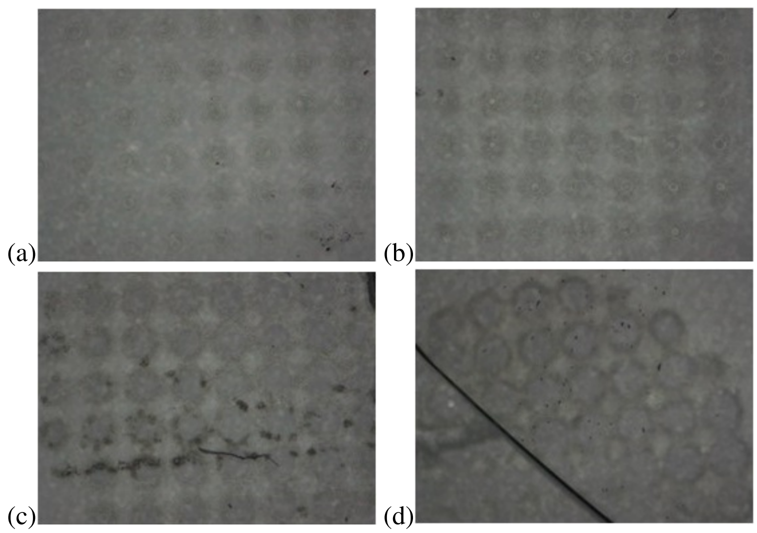

Fig. 7. Images taken with a bright field microscope of a photoresist sample exposed to a UV LED source at different time exposure(a).Exposure time of 60min.(b).Exposure time of 120min.(c).Exposure time of 180min.(d).Exposure time of 240min.

To better illustrate the results we decided to cover the developed slide of copper. The Figures 8 show the results after evaporation. The pattern exposed at 60 min has disappeared as the photoresist wasn't enough exposed to the UV source. The Figure 8b. shows the most representative expected result. The fact that each pattern is not perfectly identical is due to the incident beam that was not homogeneously distributed. To compensate this problem, replacing the UV LED source by a stronger one would have been a good option if we would have owned one.

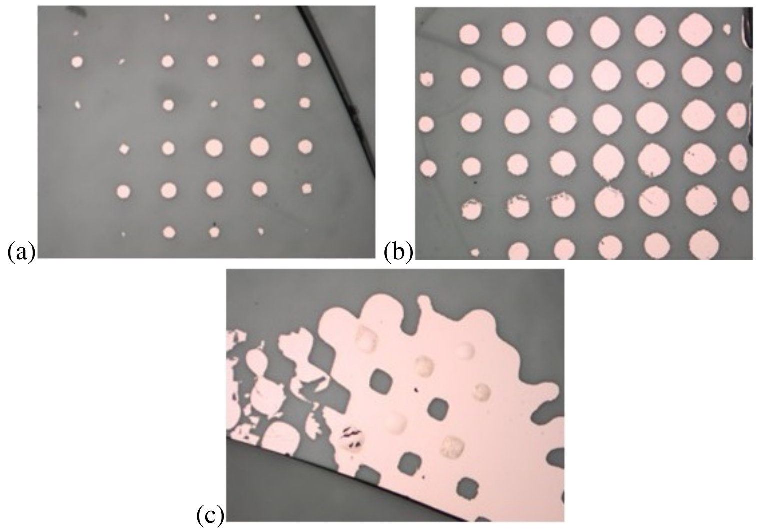

Fig. 8. Images taken with a microscope of a photoresist slide covered of copper after evaporation(a).Exposure time of 120min.(b).Exposure time of 180min.(c).Exposure time of 240min.

Another measurement was performed on an second photoresist slide. The Figure 9 shows the result obtained after a certain exposure time. In this case the sample was not enough exposed to the UV source to allow the beam to go completely through the photoresist. But we observed that the exposed photoresist had created curved rings that could be associated to microarray lens[12]. With the principle of Newton's ring we were able to estimate the surface curvature of the patterns at μm scale.

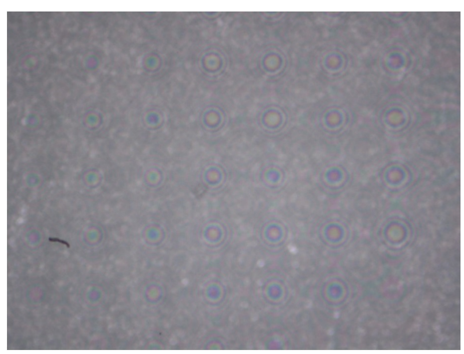

Fig. 9. Mycroscope image of a photoresist slide developed after exposure at a UV source for 90min.

4. Conclusion

The structured illumination device that we have set up presents several benefits. First of all it presents the advantage of a cheap device to build. And it is easy to provide each element. Also this device is not dependent of any electronic system. Combining this device with the photoresist method makes interesting to obtain a desired pattern on large zones on the substrates. It is also a method that allowed to create miccroarray lens. Some improvements can be done by changing the shear of the Savart Plates, with a higher shear the size of the patterns would be smaller. But also by changing the UV LED source by a stronger source, it would allow a better intensity distribution at the incident beam and so more regular and homogeneous patterns.

5. Acknowledgements

This work was funded by European Unions Horizon 2020 research and innovation programme under grant agreement No 644956, by Fundaci Privada Cellex, by Spanish Ministry of Economy and Competitiveness (MINECO), Fondo Europeo de Desarrollo Regional (FEDER) through grant TEC2013-46168-R and by NATO's Public Diplomacy Division in the framework of"'Science for Peace"'.